CLUSTER OBSERVATION OF MAGNETIC STRUCTURE AND ELECTRON FLOWS AT A NORTHWARD INTERPLANETARY MAGNETIC FIELD X-LINE

D. E. Wendel[(1)], P. H. Reiff [(1)], T. H. Han[(2)], M. L. Goldstein[(3)], E. Lucek[(4)], A. Fazakerley[(5)]

[(1)] *Rice University, Houston, TX 77005, USA, Email: dew52@columbia.edu*
[(2)] *Hong Kong University of Science and Technology, Hong Kong, P.R.China, Email: tianheng@rice.edu*
[(3)] *Goddard Space Science Center, Laboratory for Solar and Space Physics, Greenbelt, MD 20771, USA, Email: melvyn.l.goldstein@nasa.gov*
[(4)] *The Blackett Laboratory, Imperial College, London, UK, Email: e.lucek@imperial.ac.uk*
[(5)] *Mullard Space Science Laboratory, Holmbury St. Mary, Dorking, UK, Email: anf@mssl.ucl.ac.uk*

ABSTRACT

On March 18, 2002, the Cluster satellites traveled from the earth's northern mantle into the magnetosheath. During this time, the IMAGE spacecraft observed a long-lived proton emission northward of the auroral zone. The Cluster electron and magnetic field data suggest Cluster passed within 1 km of an active reconnection line, entering the ion diffusion region and the edge of the electron diffusion region. We present the current structure, velocity, orientation, and size of the reconnection line. The functional fit to the data also gives an estimate of 100 km for the thickness of the current sheet. We propose that the x-line, though wavering over the spacecraft, is globally stable during Cluster's passage through the magnetopause.

1. INTRODUCTION

The natural tendency of the southward interplanetary magnetic field (IMF) to lie anti-parallel to the earth's dipole field at the subsolar point tends to favor magnetic reconnection with a southward directed IMF. However, a northward IMF could drape upon the earth's magnetopause in a roughly anti-parallel orientation over the magnetic lobes in a manner that also allows reconnection. The advances in satellite surveillance of the sun-earth magnetic field interaction have also unearthed increasing indirect evidence for northward IMF reconnection (Fuselier, Petrinec, and Trattner [2]). Moreover, direct *in situ* multi-point observations of a reconnection site provide a rare opportunity to investigate the steadiness and spatial structure of reconnection. Many current reconnection studies focus on the length and time scales associated with ion and electron demagnetization and the role these and the resulting current structures play in the reconnection rate. In this paper we will examine this event's Cluster PEACE electron moments and FGM magnetic field data to confirm the presence of an x-line and determine its stability, motion, and magnetic structure.

2. MAGNETIC FIELD EVIDENCE FOR RECONNECTION

On March 18, 2002, from 14:54 to 15:05 UT, Cluster passed from the northern tail lobe through the magnetopause and into the magnetosheath, moving primarily along the noon-midnight meridian toward the sun (see Fig. 1). It passed through 81° latitude and 14 MLT. Phan *et al.* [5] mapped the ionospheric footprint of the spacecraft to within error of a northern reconnection spot observed simultaneously in FUV emissions by the IMAGE spacecraft for a period of 5.5 hours (Frey, et al., [1]). Phan, et al., [5] note that the velocities meet the Walèn criterion.

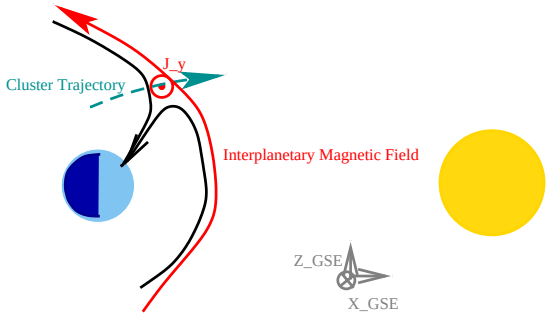

FIG. 1. Cluster passes from the northern tail lobe through the magnetopause and into the magnetosheath, moving primarily along the noon-midnight meridian toward the sun.

In Fig. 2, we present the Cluster-1 FGM (Field Gate Magnetometer) magnetic field data for the interval during Cluster's magnetopause crossing. The average magnetosphere fields are roughly anti-parallel to the average magnetosheath fields, but in the magnetopause, the GSE magnetic field components B_x and B_z simultaneously change sign several more than once, suggesting Cluster nears or crosses a magnetic null multiple times. The null near 15:00 UT presents the smallest values observed and thus the closest possible approach to an x-line. Because the

magnetopause has about a 67° tilt from GSE x, we perform all further analysis in a coordinate system aligned with the magnetopause.

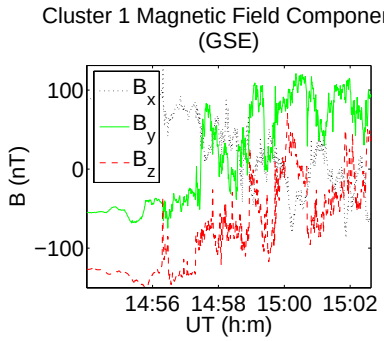

FIG. 2. Cluster-1 FGM magnetic field data for the interval during Cluster's magnetopause crossing. Cluster crosses several magnetic nulls in the B_x and B_z components.

The enhancements in B_y that just precede the magnetic nulls in B_x and B_z might result from Hall currents. A superposition of B_y and the components of the current derived from the magnetic field estimates, or the curlometer current, as discussed in section 3, supports this conclusion (see Fig. 3). The position of Cluster 2 at the edge of the discontinuity in B_y therefore suggests an ion diffusion box half-width of about 110 km. Simulations put the Hall current region to within about 10 ion skin depths λ_i of the x-line, where $\lambda_i = c/\omega_i$ (Shay, Drake, and Rogers [7], Hesse, Birn, and Kuznetsova [4]). Calculations of the ion skin depth from measurements of ion density in the magnetopause yield $\lambda_i = 24$ km and an ion diffusion half-width of 240 km, so that the distance we propose between Hall currents and the x-line lie well within this limit.

As a formal check for rotational discontinuities in the magnetic field data, we apply an algorithm, developed by Hausman and Michel, [3], that is insensitive to tangential discontinuities, i.e.,

$$\rho = (\boldsymbol{B}_1 \times \boldsymbol{B}_2) \cdot \boldsymbol{B}_3, \qquad (1)$$

where $\boldsymbol{B}_1$, $\boldsymbol{B}_2$, and $\boldsymbol{B}_3$ are sequential measurements of the magnetic field. (In our case the FGM data has .25 s resolution and we have smoothed it by a triangular average.) Fig. 4 depicts the three components of the magnetic field along with the quantity ρ, the black curve. The small oscillations in ρ are noise, but the large spikes signify rotational discontinuities. Note that these occur where the B_x, B_z components approach zero magnitude and B_y experiences a sudden enhancement, which corroborates that Cluster is traveling through reconnection site rotational discontinuities at these times.

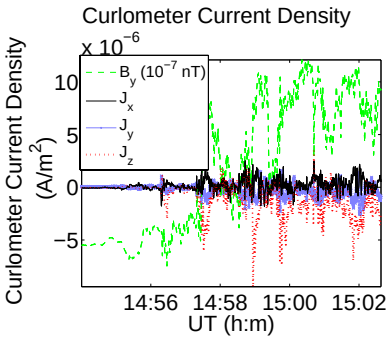

FIG. 3. The large curlometer currents measured in the z direction (and, to a lesser extent, in the x direction) of discontinuities in the magnetic field data strengthens the case for Hall currents.

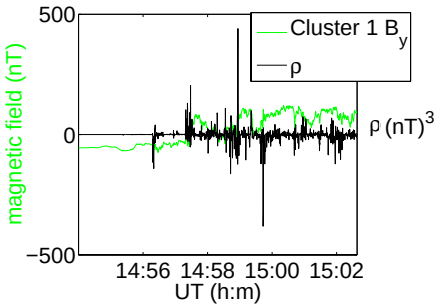

FIG. 4. The y component of the magnetic field along with the measure of rotational discontinuity, ρ, in black.

3. ELECTRON EVIDENCE FOR RECONNECTION

The superposed-epoch electron moments at the x-line are depicted in Fig. 5 along with the derived magnetic field model there (light arrows signify vectors with a negative y-component, and dark arrows vectors with a positive y-component). There is a pattern of inflow and accelerated outflow at the x-line in the x-z plane. Moreover, the positive-y flows (corresponding to the negative-y reconnection current sheet) are centered within roughly 100 km of the x-line, consistent with the current sheet thickness estimated later in the paper. The electron moments at the x-line give a current density on the order of $J_y \sim 10^{-6}$ A/m^2, the same order of magnitude as the current sheet density obtained by taking the instantaneous curl of the magnetic field measured by the four spacecraft (the "curlometer" current). (The ions are moving at ~ 50 - 150 km/s in the region around the x-line). Furthermore, the Alfvén speed is roughly 276 km/s for the local ion density (~ 90/cm^3), using an asymptotic magnetic field of 120 nT, while the electron flows are approximately 300-400 km/s within a few km of the inferred reconnection site. The first-order electron moments in the vicinity of the x-line are therefore consistent with the normal inflows and tangential outflows that define a reconnection region, with currents derived from the

magnetic field data, and with the supra-Alfvénic speeds observed in the ion demagnetization region of reconnection simulations (Hesse, Birn, and Kuznetsova [4]).

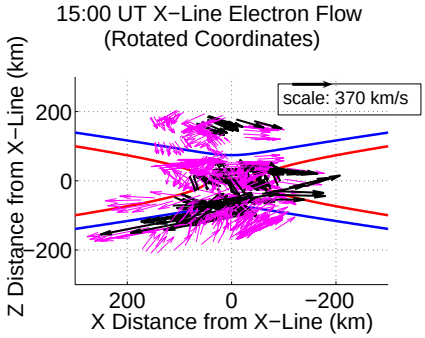

FIG. 5. Superposed epoch electron flow vectors (black and grey arrows) near the x-line at 15:00 UT. Grey arrows signify vectors with a negative y-component, and black arrows vectors with a positive y-component.

The second-order electron moments further support the proximity of a reconnection line. The electron skin depth for the density observed in the magnetopause is about 1 km, so our x-line distance measurements suggest we may not penetrate the electron diffusion region. However, when we pass within 1 km or 3.5 km of the x-line (as Cluster 2 and Cluster 4 do, respectively) we are close enough to at least view effects of partial demagnetization in the transition region. This is a transition region between the ion and electron diffusion regions that lies within an ion gyroradius of the reconnection site. The electron pressure divergence and shear support this. Moreover, the contribution to Ohm's law reaches a maximum of 12 mV/m in the negative y-direction at 15:00 UT.

For example, at 15:00 UT, the off-diagonal P_{xy} terms of the pressure tensor rotated to the magnetopause-aligned coordinate system (Fig.6) have the structure expected in an x-line diffusion region. As explained by Vasyliunas [8], symmetry of the velocity distributions about the x-line makes P_{xy} vanish at the x-line. P_{xy} also approaches zero at the edge of the diffusion region because the growing gyromotion about a larger B_z essentially magnetizes the electrons and increases axial symmetry about the z-direction. Thus the off-diagonal terms P_{xy} diminish (Vasyliunas [8]). The sign of P_{xy} is also consistent with the negative B_z component accelerating an electron moving in the positive y-direction into the positive x-direction (in the magnetopause-aligned coordinate system).

The enhanced Lorentz acceleration perpendicular to the field direction causes an asymmetry of particlesalready accelerated by the reconnection electric field in the other perpendicular direction (Hesse, Birn, and Kuznetsova [4] and Scudder *et al.* [6]). As discussed regarding Fig. 6, we observe a similar enhancement in the P_{xy} component in a field-aligned coordinate system (Fig. 7). We do see some enhancement—16% of the diagonal pressure—of the off-diagonal (shear) terms in the magnetopause-aligned (Fig. 6) and the field-aligned (Fig. 7) pressure near the purported x-line at 15:00 UT. This shear can only develop when the particles are partially demagnetized, since the shear reflects that some particles are moving differentially from the bulk flow with respect to the magnetic field (Hesse, Birn, and Kuznetsova [4]).

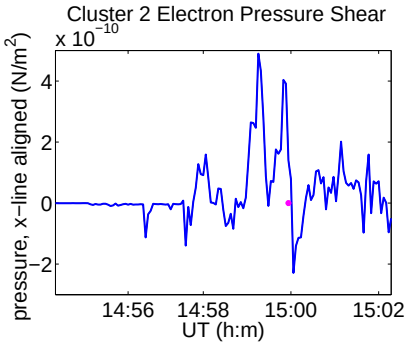

FIG. 6. This figure, extracted from Cluster 2 data, demonstrates that the pressure tensor off-diagonal components, particularly P_{xy}, increase and vary in the manner expected near an x-line (position of 15:00 UT denoted by the star).

The divergence term $(\nabla \bullet \boldsymbol{P})/n_e e$ (Fig. 8) reaches 15% of the maximum Hall electric fields in the region around the x-line, a strong indicator of the proximity of the electron diffusion region. Hesse, Birn, and Kuznetsova [4] achieve a maximum reconnection E_y of $.3 v_A B_0$, where v_A and B_0 are the asymptotic Alfvén speed and magnetic field, respectively. This presents an order-of-magnitude estimate, as the authors note that the value drops in time. For our asymptotic field and density values of $B_0 \approx$ 120 nT and $n_{p0} \approx 9\text{x}10^7/\text{m}^3$, $.3 v_A B_0 \approx$ 10 mV/m, satisfyingly close to our pressure divergence contribution of 12 mV/m. Note that we calculate the pressure divergence instantaneously by a least-squares estimate from data collected by all four spacecraft.

Finally, over the width of the magnetopause, the electron scalar pressure scales inversely with the magnetic pressure in the manner expected of reconnecting fields. The log-log hodogram of this relationship, depicted in Fig. 9, is further evidence for a spatially coherent and temporally continuous reconnecting layer that is wavering with respect to the spacecraft (*Scudder*, *et al.*, [6]). The plasma β is on the order of unity throughout the magnetopause crossing, at times reaching values of 1-2. The fact that B_y does not vanish at the locations where Cluster passes close to the x-line prevents the plasma β from reaching very large values ($\beta >> 1$) at those points.

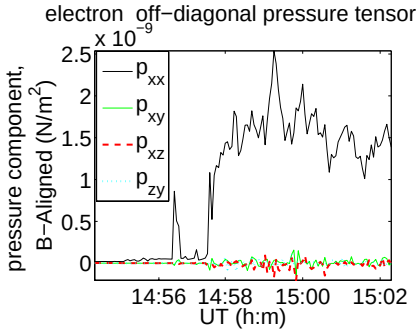

FIG. 7. The pressure diagonal (above) and off-diagonal (below) components in a field-aligned coordinate system. The diagonal term P_{xx} is included below for comparison. The shear terms reach 16% of the diagonal terms near the x-line at 15:00 UT (marked by an asterisk above).

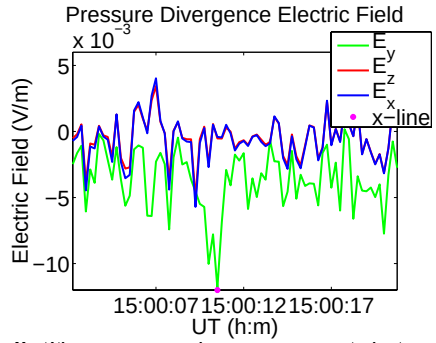

FIG. 8. The pressure divergence contribution to the electric field E_y at 15:00 UT attains a value that is 15% of the Hall electric field contribution.

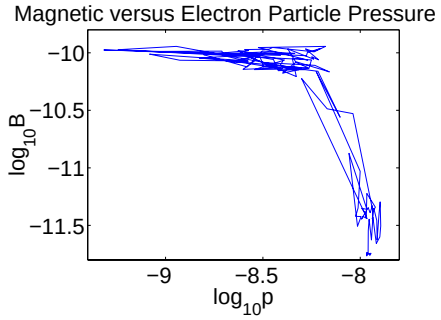

FIG. 9. A log-log relationship between magnetic pressure (vertical axis) and particle pressure (1/3trace(***P***), horizontal axis) for the entire magnetopause crossing. The inverse relationship signifies a nearby separator line.

4. X-LINE MOTION

An inversion of the Taylor expansion for the B_x and B_z components yields the spacecraft distance from the x-line. We assume that the line is nearly along the y-direction (hence $dy = y - y_{xl} = 0$) for a spacecraft crossing the x-line):

$$B_x = \left(\frac{\partial B_x}{\partial x}\right)\Big|_{xl}(x - x_{xl}) + \left(\frac{\partial B_x}{\partial z}\right)\Big|_{xl}(z - z_{xl})$$
$$B_z = \left(\frac{\partial B_z}{\partial x}\right)\Big|_{xl}(x - x_{xl}) + \left(\frac{\partial B_z}{\partial z}\right)\Big|_{xl}(z - z_{xl}) \qquad (2)$$

The spatial derivatives are evaluated at the centroid's closest approach to a minimum B_x and B_z by way of a multi-spacecraft least squares fit of $\partial B_i/\partial x_j$, while B_i is evaluated at the x-z position of each spacecraft at closest approach to minimum B_x and B_z. From the spacecraft distance to the x-line we calculate the x-line position as a function of time.

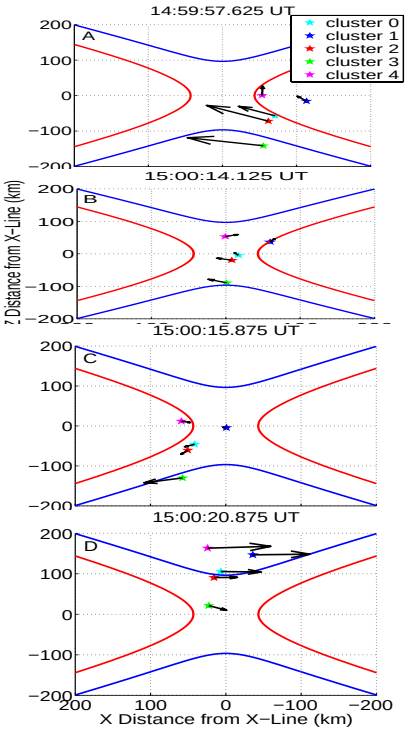

FIG. 10a-10d, (top to bottom). Frames from a movie modeling the spacecraft motion relative to the x-line near 15:00 UT, in the x-line reference frame. We include a model of the zeroth-order x-line magnetic field lines. The magnetic field vectors at each spacecraft are depicted as black arrows.

The estimated x-line positions (x_{xl}, z_{xl}) allow us to estimate and remove the x-line velocity. The spacecraft frame x-line velocity is necessary to derive an accurate current sheet width from the centroid's spatial gradient estimations, and to determine the steadiness and spatial continuity of the reconnection site. From

measurements of x-line positions and times at the null crossing near 15:00 UT, a least-squares fit of the x-line velocity estimates a moderate rate tailward and earthward of v_x = .8 km/s and v_z = -6 km/s. Cluster 2 penetrates as close as at least 1 km from the x-line and Cluster 4 within about 3.5 km. The x-line continues to jitter at later crossings: at 15:01, the x-line slides away from earth at a rate v_x = -2 km/s, v_z = 7.6 km/s; at 15:02, the x-line moves inward again at v_x = 7.2 km/s, v_z = -10.4 km/s and cluster is on the sheath side of the fields; and at 15:03, it sweeps very rapidly back toward earth at v_x = 7.4 km/s, v_z = - 44 km/s—note the steepness of the magnetic field gradient at that time. The motion is consistent with a single, oscillating x-line, but we cannot rule out the possibility that we encounter multiple x-lines from a tearing-mode instability.

5. SPATIAL AND TEMPORAL STRUCTURE OF RECONNECTING MAGNETIC FIELDS

Fig. 11a-11b are statistical maps of B_x and B_z at the positions of all spacecraft (including the centroid) relative to the x-line in a 30-s time window around the 15:00 UT crossing. The positions of the spacecraft relative to the x-line are determined from the Taylor expansion of the previous section, while the magnetic field values come from the data. These maps allows us to fit the magnitude and distance parameters B_o and Δ, respectively, of a Harris sheet model, i.e.,

$$B_x(z) = B_0 \tanh(z/\Delta) . \qquad (3)$$

The fit is shown by the curve in the figures. The Harris sheet is general enough to describe the x-line positions and velocities at distances where the Taylor expansion may be invalid. Note that in both figures the statistics favor a pronounced linear fit through the origin, which we exploit to remove the uncertainty in the gradient used in the Taylor expansion of the preceding section. Thus the final positions of the spacecraft relative to the x-line follow from a second iteration. The fit to B_x gives an absolute current sheet thickness, since we have derived it in the x-line frame of reference. If the operational definition of the current sheet thickness is full-width at half-maximum, then the value of Δ = 50 km in Fig. 11a implies a current sheet thickness of 100 km. The fit to the $B_z(x)$ data in Fig. 11b yields a significant asymptotic reconnection B_z of approximately 10 nT. Such a normal field would produce a polar cap potential drop of about 77 kV, given a polar cap width of 3 earth radii and an anti-sunward solar wind speed of 400 km/s.

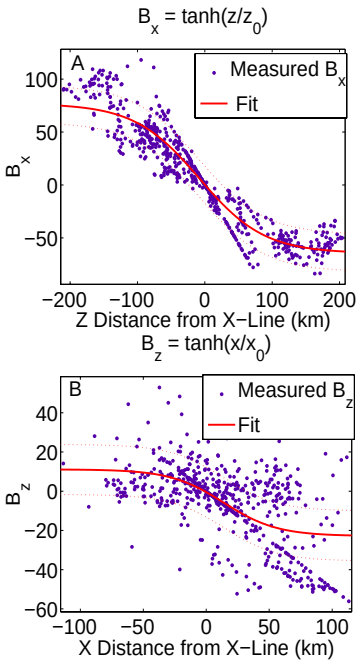

FIG. 11a-11b. A statistical map of B_x as a function of z (above) and B_z as a function of x (below) (the centroid is included). The figures include all times in a 30 s interval around 15:00 UT.

6. CONCLUSIONS

For the case of a northward IMF, we observe wavering but otherwise steady reconnection magnetic B_x, B_z fields, and an induced B_y, that are consistent with an anti-parallel merging site twisting through the out-of-plane (y) direction. Fig. 12 represents the geometry as well as the fact that conjugate reconnection is most likely occurring simultaneously. The observation of bi-directional field-aligned electron flows suggests the latter. The resulting potential field drop mapped to the ionosphere is consistent with anti-sunward convection flows. We find that there is a steep interior field: the orientation of the lobe and draping at the reconnection site is tilted at ~ 67 ° from the GSE horizontal. We use distance-to-x-line estimates to assess the x-line motion, and determine that it is consistent with a single, steady x-line wavering across the spacecraft at speeds in the range of ≈ 6 to 45 km/s. However, we cannot rule out encounters with multiple x-lines from a tearing mode instability. Resistance to slippage at a tailward location adjacent to the magnetosheath is consistent with Phan *et al.*'s [5] observation of a plasma depletion layer (PDL) at the same time and location. Fuselier, Petrinec and Trattner [2] have found that a larger magnetic field and lower density in a PDL produces sub-Alfvénic flow adjacent to the magnetopause, which is consistent with a relatively steady x-line position. Analysis of the magnetic field gradients shows that the Cluster spacecraft come within 1 km of the x-line. This means we have passed through at least the outflow and the ion

diffusion regions, the current sheet, and perhaps the electron partial demagnetization region, on our way through the magnetopause. Statistical fitting of a Harris sheet model yields a current sheet thickness estimate of approximately 100 km. We infer an ion diffusion region that is at least as large as roughly 220 km thick, on the basis of detecting the edge of the Hall current region at the perpendicular electron flows. This estimate agrees with a Hall zone within $10\lambda_i$ of the x-line, as predicted by the simulations in other papers. The off-diagonal pressure components and the pressure gradients are sympathetic with proximity to the electron diffusion region. The pressure shear terms attain values about 15% of the diagonal pressure valuesnear the x-line. In the absence of Cluster electric field data, we compare the pressure divergence contribution to E_y with the magnitude of the Hall term in Ohm's law, presumed significant in the ion diffusion region, as well as simulation estimates of E_y. The 12 mV/m pressure divergence reaches 15% of the maximum Hall term magnitudes in the region, and agrees well with simulation estimates by Hesse, Birn, and Kuznetsova [4]. Very near the x-line the electron flow becomes aligned with the electric field, suggesting that Cluster might have reached the electron diffusion layer.

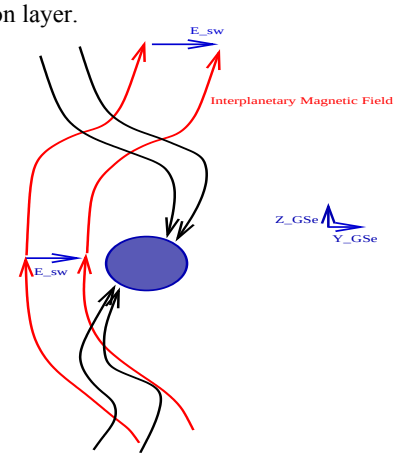

FIG. 12. Reconnection magnetic B_x, B_z field, with an induced B_y, that is consistent with an anti-parallel merging site twisting through the out-of-plane (y) direction.

Acknowledgements

The authors thank Steven Schwartz for his calibrated electron moments and advice. This research is supported in part by NASA under grant NAG5-13219.

References

1. H. U. Frey, T. D. Phan, S. A. Fuselier, and S. B. Mende, Continuous Magnetic Reconnection at Earth's Magnetopause, *Nature,* Vol. 426, 533-536, 2003.

2. S. A. Fuselier, S. M. Petrinec, and K.J. Trattner, Stability of the High-Latitude Reconnection Site for Steady Northward IMF, *Geophys. Res. Lett*., Vol. 27, 473-476, 2000.

3. Hausman, B. A., F. C. Michel, J. R. Espley, and P. A. Cloutier, On Determining the Nature and Orientation of Magnetic Directional Discontinuities: Problems with the Minimum Variance Method, *J. Geophys. Res.,* Vol. 109, A11102, 2004.

4. Michael Hesse, Joachim Birn, and Masha Kuznetsova, Collisionless Magnetic Reconnection: Electron Processes and Transport Modeling, *J. Geophys. Res.,* Vol. 106, 3721-3735, 2001.

5. T. D. Phan *et al.*, Simultaneous Cluster and IMAGE Observations of Cusp Reconnection and Auroral Proton Spot for Northward IMF *Geophys. Res. Lett.,* Vol. 30, 1509 (2003).

6. J.D. Scudder, F. S. Mozer, N.C. Maynard, and C. T. Russell, Fingerprints of Collisionless Magnetic Reconnection at the Separator, I, Ambipolar-Hall Signatures, *J. Geophys. Res.,* Vol. 107, 1294-, 2002.

7. M. A. Shay, J. F. Drake, and B. N. Rogers, The Scaling of Collisionless, Magnetic Reconnection for Large Systems, *Geophys. Res. Lett.,* Vol. 26, 2163-2166, 1999.

8. Vytenis M. Vasyliunas,, Theoretical Models of Magnetic Field Line Merging, 1, *Rev. Geophys. And Space Phys.,* Vol. 13, 303-336.